Nonlinear Ballistic Response of Quantum Spin Hall Edge States

Pankaj Bhalla,[1,2,3] Ming-Xun Deng,[4,5] Rui-Qiang Wang,[4,5] Lan Wang,[6,7] and Dimitrie Culcer[3,2]
[1]Beijing Computational Science Research Centre, Beijing 100193, China
[2]ARC Centre of Excellence in Future Low-Energy Electronics Technologies, The University of New South Wales, Sydney 2052, Australia
[3]School of Physics, The University of New South Wales, Sydney 2052, Australia
[4]Guangdong Provincial Key Laboratory of Quantum Engineering and Quantum Materials, Guangzhou 510006, China
[5]South China Normal University, Guangzhou 510006, China
[6]School of Science, RMIT University, Melbourne, Victoria 3000, Australia
[7]ARC Centre of Excellence in Future Low-Energy Electronics Technologies, RMIT Node, RMIT University, Melbourne, Victoria 3000, Australia

(Received 30 July 2021; accepted 15 October 2021; published 8 November 2021)

Topological edge states (TES) exhibit dissipationless transport, yet their dispersion has never been probed. Here we show that the nonlinear electrical response of ballistic TES ascertains the presence of symmetry breaking terms, such as deviations from nonlinearity and tilted spin quantization axes. The nonlinear response stems from discontinuities in the band occupation on either side of a Zeeman gap, and its direction is set by the spin orientation with respect to the Zeeman field. We determine the edge dispersion for several classes of TES and discuss experimental measurement.

DOI: 10.1103/PhysRevLett.127.206801

Introduction.—Topological materials such as topological insulators, Weyl semimetals, and transition metal dichalcogenides, are novel quantum materials hosting helical or chiral spin-momentum locked states on their surfaces and edges [1–15], which may enable dissipationless transport. This fact, coupled with the possibility of electrically driven topological phase transitions [16–19] has led to an explosion of interest in topological edge state transistors as novel, power-saving building blocks for next-generation integrated circuits [17,20–25]. The first step in this road map is achieving reliable ballistic samples, in which the electron mean free path l is much greater than the length d of the channel. The corresponding conduction picture is frequently described by the Landauer-Buttiker formalism [26–45].

The ballistic regime can exhibit linear as well as nonlinear transport, as observed in quantum point contacts, three-terminal ballistic branches, asymmetric microjunctions and related structures [34,46–59]. The transport properties of conventional devices such as quantum point contacts are typically tailored by device geometry in a similar fashion to the transmission properties of a waveguide [60]. On the other hand, topological edge states are expected to exhibit inversion symmetry breaking terms intrinsic to the edge Hamiltonian, which itself should enable a nonlinear electrical response in the technologically relevant ballistic regime, without additional structure inversion symmetry built into the device. Nevertheless this nonlinear phenomenon has not been considered to date, in fact the presence of inversion-symmetry breaking terms in the dispersion has never been probed, because the standard tools for this, angle-resolved photoemission and scanning tunneling microscopy, do not work for single edges. This knowledge gap motivates us to develop here a quantum kinetic theory for the nonlinear response of ballistic topological edge states. We focus on the simplest, but experimentally most relevant, case of a single channel with perfect transmission to the contacts. We find the nonlinear contribution to the current

$$j^{(2)} = (e^3/h)(V_L - V_R)^2[f'(E_Z - \mu) - f'(E_Z + \mu)]. \quad (1)$$

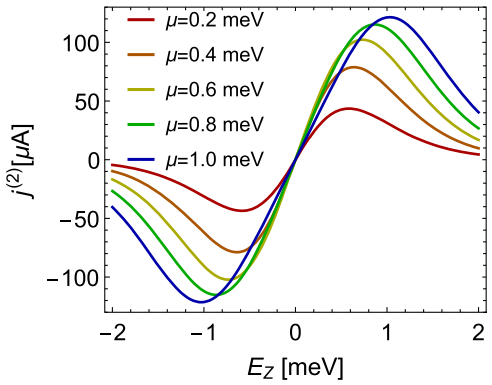

FIG. 1. Second-order response of quantum spin-Hall edge states in the ballistic regime in response to a potential difference between the left and the right electrodes at a finite Zeeman energy E_Z (meV) for different chemical potentials μ (meV) at a fixed low temperature $T = 5$ K.

This is the central result of our work. Here $f'(E_Z-\mu)$ is the derivative of the Fermi Dirac distribution function $[1+e^{\beta(E_Z-\mu)}]^{-1}$ with respect to the Zeeman energy E_Z, with $\beta=1/(k_BT)$, k_B the Boltzmann constant, T the absolute temperature, while μ is the chemical potential, and V_L (V_R) is the potential of the left (right) electrode.

Moreover, it is nonzero only due to the asymmetry created by the Zeeman energy as illustrated in Fig. 1. Here we have plotted the second-order current as a function of the Zeeman energy and the chemical potential referring the experimental setup shown in Fig. 2. It is observed that $j^{(2)}$ follows the smeared δ-function shape due to the wave vector derivative of the Fermi function. Note that for vanishing Zeeman energy, the current becomes zero. The response is unidirectional, with the direction set by the spin orientation with respect to the magnetic field, and has opposite signs on the two edges. The nonlinear part of the current changes sign on reversing the direction of the Zeeman term. The necessity of a Zeeman field reflects the fact that, beyond the linear regime, the role of time-reversal symmetry is nontrivial [61–69]. It is consistent with the recent finding that a nonreciprocal current requires time-reversal symmetry breaking either by magnetic order at the microscopic level or by incorporating irreversibility at the macroscopic level [70]. In the presence of time-reversal symmetry, the symmetrical shift in the electronic band structure in the valence and conduction bands due to the potential gradient between two electrodes nullifies the net motion of the carriers [70,71].

In order to make concrete experimental predictions, below we evaluate the ballistic nonlinear edge response for several classes of topological materials such as Na_3Bi, Bi_2Se_3, HgTe, WTe_2 and quantum anomalous Hall edge states. Our main conclusions are (i) unlike linear response, the nonlinear response can ascertain the presence of symmetry-breaking terms in the dispersion, an important step forward considering that the dispersion of topological edge states has never been probed; (ii) the shape of the nonlinear response as a function of chemical potential and Zeeman energy does not depend on the details of the band structure. Yet the response only occurs if mirror-symmetry

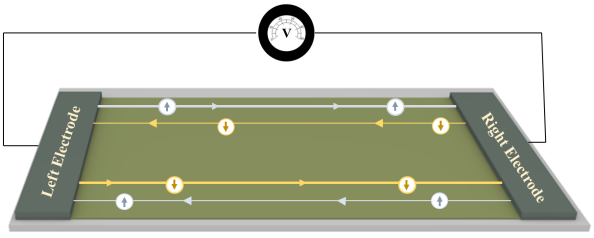

FIG. 2. Schematic of the experimental setup for measuring the nonlinear current. The voltages are measured along the left and right electrodes. Here the edge states occur in pairs having spin-up (blue) and spin-down (yellow). Thick lines refer to occupied states and thin lines to unoccupied states.

breaking terms are present in the band structure. Hence if a ballistic nonlinear response exists, it has the shape of Fig. 1; (iii) physically, the nonlinear response arises when there is a discontinuity in the linear current. To detect a finite nonlinear electrical response one straightforwardly tunes the chemical potential through the Zeeman gap, whether at the origin or at finite wave vector, while monitoring the voltage at twice the applied frequency. (iv) Although Zitterbewegung terms are formally present in the response we find they have no physical consequences in one dimension, and the Berry connection does not play a role in ballistic transport.

Quantum kinetic theory.—We begin with the quantum Liouville equation for the density operator $\hat{\rho}$,

$$\frac{\partial\hat{\rho}}{\partial t}+\frac{i}{\hbar}[\hat{H},\hat{\rho}]=0, \tag{2}$$

where $H=H_0+V$ is the full Hamiltonian of the system, with H_0 the edge state Hamiltonian and $V(x)$ the applied electrostatic potential. Projecting this equation onto the eigenstate basis of H_0 and performing a Wigner transformation [72,73], as described in the Supplemental Material [74], we obtain for the Wigner function $f\equiv f(k,x,t)$ [75–78]

$$\frac{\partial f}{\partial t}+\frac{i}{\hbar}[H_0,f]+\frac{1}{2}\left\{v,\frac{\partial f}{\partial x}\right\}=\mathcal{D}. \tag{3}$$

The Wigner function $f\equiv f(k,x,t)$ plays the role of a (matrix) distribution and is a matrix in the band representation, while $v=\hbar^{-1}(\partial H_0/\partial k-i[\mathcal{R}_k,H_0])$ is the velocity, $\mathcal{R}_k=\langle u_k|i\nabla|u_k\rangle$ is the Berry connection with $|u_k\rangle$ the lattice-periodic part of the Bloch function, and the driving term $\mathcal{D}=-e/\hbar\partial V/\partial x(\partial f/\partial k-i[\mathcal{R}_k,f])$. It is convenient to take the Fourier transform (FT) of Eq. (3) with respect to space and time,

$$-i\omega\tilde{f}+\frac{i}{\hbar}[H_0,\tilde{f}]-\frac{iq}{2}\{v,\tilde{f}\}=\tilde{\mathcal{D}}(q,\omega), \tag{4}$$

where $\tilde{f}(k,q,\omega)$ depends on the pseudomomentum q. The driving term $\tilde{\mathcal{D}}$ is independent of time, thus the time FT results in $\tilde{\mathcal{D}}(q,\omega)\propto\delta(\omega)\tilde{\mathcal{D}}(q)$ which will contribute only at $\omega=0$. Because of this, we neglect the frequency dependence of $\tilde{f}(k,q)$. We decompose the matrices in terms of the 2×2 Pauli basis as $\tilde{f}=\tilde{S}_0\mathcal{I}+\tilde{S}_1\sigma_x+\tilde{S}_2\sigma_y+\tilde{S}_3\sigma_z$, $v=v_0\mathcal{I}+v_1\sigma_x+v_2\sigma_y+v_3\sigma_z$, where $\tilde{S}_i$, and v_i represent the components of the Wigner function and the velocity associated with the corresponding Pauli matrices σ_i, respectively. Since we are working in the energy eigenstate basis the edge Hamiltonian $H_0=\varepsilon_0\mathcal{I}+\varepsilon_3\sigma_z$, with ε_i labeling the two (matrix) components of the dispersion. This decomposition leads to a set of four equations corresponding to the identity matrix and

three Pauli matrices. The resulting equations can be expressed in matrix form as $\tilde{\mathcal{M}}\tilde{f} = \tilde{\mathcal{D}}$, where $\tilde{\mathcal{M}}$ is a 4×4 matrix, given in the Supplemental Material [74]. Transforming back to real space yields the convolution structure

$$f(k,x) = \int dx' \mathcal{M}^{-1}(x-x')\mathcal{D}(x'). \tag{5}$$

Inserting the expressions for v, and f, one can find the current using the definition [73], $j = -e\mathrm{Tr}(vf)$ to Nth order of the potential (Tr being the full operator trace)

$$j^{(N)} = -\frac{e^2}{h}\int_0^x dx' \frac{\partial V}{\partial x'} p(x') + \frac{e^2}{h}\int_d^x dx' \frac{\partial V}{\partial x'} p(x'). \tag{6}$$

Here the x integral is for the length of the channel where the potential is intact, $p(x') = [S_0^{(N-1)}(x,x')]_{k=0}$, where $S_0^{(N)}(x,x') = M_{11}^{-1}(x-x')\mathcal{D}_0^{(N)}(x') + M_{12}^{-1}(x-x')\mathcal{D}_1^{(N)}(x') + M_{13}^{-1}(x-x')\mathcal{D}_2^{(N)}(x') + M_{14}^{-1}(x-x')\mathcal{D}_3^{(N)}(x')$ and d is the length of the channel. The direct contributions stemming from other elements of the density matrix such as S_1, S_2, and S_3 cancel out due to the cancellation of terms after taking the product of the matrix elements of the $\mathcal{M}^{-1}(x)$ with the velocity components, thus do not contribute to the main expression for the nonlinear current. However, the indirect contributions of such terms still survive through the driving terms. The detailed derivation of Eq. (6) is given in the Supplemental Material [74]. Further, in Eq. (6), the first term is for the carriers moving towards the right side of the electrode or right movers and the second term for the left movers. For the linear order or $N = 1$, the quantity $p(x)$ reduce to $S_0^{(0)}$ which is the equilibrium part of the density matrix and it is equivalent to f_0^s, where $f_0^s = f_0(\varepsilon^+) + f_0(\varepsilon^-)$ is the sum of the equilibrium distribution functions at the energies correspond to the conduction (+) and the valence (−) bands. The distribution function is independent of the space variable, thus can be pulled out from the integrand and the spatial integration over x can be performed easily. The latter results the linear current as $e^2/h(V_L - V_R)f_0^s$. At the low temperature and when the chemical potential lies in one of the bands, the current becomes $e^2/h(V_L - V_R)$. This is consistent with the Landauer-Buttiker formula for the conductance [27,35]. However, if the chemical potential lies in the gap between the valence and conduction bands, the current vanishes.

In the nonlinear regime or the second-order case, the current becomes proportional to the first power of the density matrix $S_0^{(1)}$ at $k = 0$. The latter quantity using the definitions for the driving terms can be written as $S_0^{(1)}(x,x') = \partial V/\partial x'[M_{11}^{-1}(x-x')\partial f_0^s/\partial k + M_{12}^{-1}(x-x')\mathcal{R}_2 f_0^d + M_{13}^{-1}(x-x')\mathcal{R}_1 f_0^d + M_{14}^{-1}(x-x')\partial f_0^d/\partial k]$, where f_0^d refers to the difference between the equilibrium distribution function at different bands. To solve the space integral, it is convenient to split the matrix elements into two parts $M_{ij}^{-1}(x) = [M_{ij}^{-1}]_a + [M_{ij}^{-1}]_b e^{-xg(k)}$, having the first part of the element as space independent while the other part depends. The forms of different elements of the inverse of the matrix $\mathcal{M}$ are mentioned in the Supplemental Material [74]. Here

$$g(k) = \sqrt{\frac{(v_3^2 - v_0^2)\varepsilon_3^2}{\hbar^2 v_0^2(v_0^2 - v_1^2 - v_2^2 - v_3^2)}} \tag{7}$$

determines the Zitterbewegung or decaying nature of the current depending on the strengths of the velocity components. However, in the present study we find that at $k = 0$ the terms associated with the exponential factor approaches to zero due to the diverging nature of $g(k)$ for a model having finite value of the component of the velocity v_0. In other cases, this term does not appear in the matrix elements, and we can drop it in the remaining analysis. The general expression for the ballistic second-order current is

$$j^{(2)} = \frac{e^3(V_L - V_R)^2}{h}\left(M_{11}^{-1}\frac{\partial f_0^s}{\partial k} + M_{14}^{-1}\frac{\partial f_0^d}{\partial k}\right)_{k=0}. \tag{8}$$

Hamiltonian.—We consider a generic edge of finite length d which is described by the total Hamiltonian $H = H_0 + H_Z + V(x)$, where H_0 is the Bloch band Hamiltonian corresponding to the edge dispersion of the system under consideration, H_Z is the Zeeman energy term, and $V(x)$ the applied potential difference. We briefly sketch the derivation for the edge state Hamiltonian for Bi_2Se_3 within the $\boldsymbol{k}\cdot\boldsymbol{p}$ theory framework [79]. We start with the effective 4×4 Hamiltonian for Bi_2Se_3 in the basis $\{\psi_{c\uparrow}, \psi_{v\uparrow}, \psi_{c\downarrow}, \psi_{v\downarrow}\}$ which has the block diagonal form

$$H = \begin{pmatrix} h_+(\boldsymbol{k}) & 0 \\ 0 & h_-(\boldsymbol{k}) \end{pmatrix}. \tag{9}$$

Here the block matrices $h_\pm = E_0\mathcal{I} + D_0(k_x^2 + k_y^2)\mathcal{I} + \lambda(k_x^3 - 3k_x k_y^2)\sigma_z - \alpha k_\mp \sigma_y$, where the second term, which is the quadratic term in the wave vector, refers to the kinetic energy term having D_0 as a material-dependent parameter, the third term is for the warping which reduces the infinite mirror planes to three [80] whose strength is considered by the warping coefficient λ, and the last term represents the spin-orbit interaction having α a spin-orbit coupling constant, E_0 is a constant term, and $k_\pm = k_x \pm ik_y$, where k_x (k_y) is the component of the wave vector along the $\hat{x}$ ($\hat{y}$) direction. To obtain the Hamiltonian for the edge states, we consider a finite size system that is placed in the x-y plane and is defined between the boundaries as $-d/2 < y < d/2$ along the $\hat{x}$ direction. Because of the broken translational symmetry for the $\hat{y}$ direction, the wave vector k_y needs to be

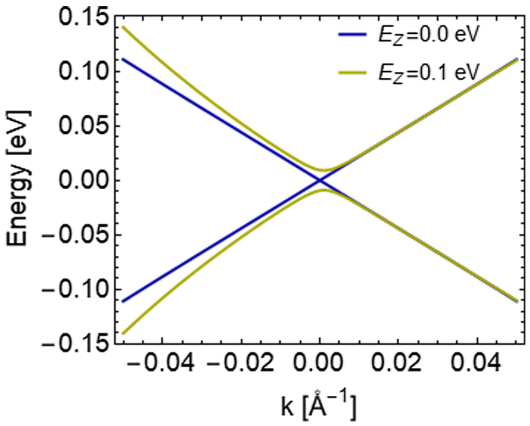

FIG. 3. Edge energy dispersion for Bi_2Se_3 with the Zeeman energy term, but without the particle-hole symmetry term at fixed warping coefficient $\lambda = 100$ eV Å^3.

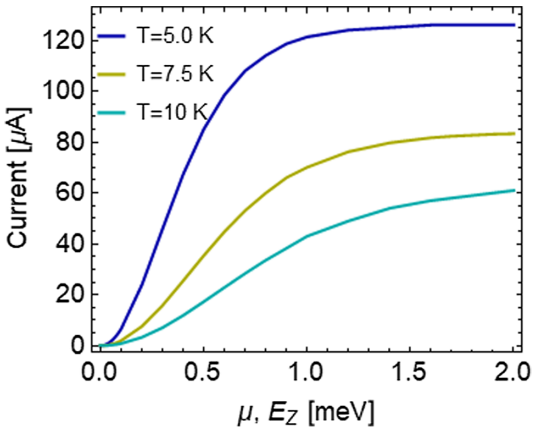

FIG. 4. Nonlinear current as a function of the chemical potential (μ), which is set equal to the Zeeman energy (E_Z) at different low temperature values: 5, 7.5, and 10 K.

replaced by an operator $-i\partial_y$ and the eigenvalue equation for the upper and lower block matrix separately using the Schrodinger equation $h_s(k_x, -i\partial_y)\Phi_0^s = E_s\Phi_0^s$ has been solved where $\Phi_\kappa^s = e^{ik_x x}e^{\kappa y}\psi_s$ is the edge wave function for the above Hamiltonian having κ as real numbers, and $s = +1$ (-1) for the upper, $\uparrow$ (lower, $\downarrow$) block. In principle, the resulting calculation is too complex and it is difficult to obtain the analytical expressions. To proceed, we first solve the edge wave function in the limit $\lambda \to 0$ and project the total Hamiltonian onto these edge wave functions $\{\psi_0^{\uparrow,\gamma}(r), \psi_0^{\downarrow,\gamma}(r)\}$ with $\gamma = \pm$. We find that the Hamiltonian yields the dispersion $\varepsilon_\pm = E_0 \pm \alpha k_x \sigma_z$. Then, we find the elements of the effective edge Hamiltonian along the $\hat{x}$ direction using $H_{\text{edge}}^{\gamma ss'} = \langle \tilde{\Psi}_0^{s,\gamma}(r)|h_s(k_x, -i\partial_y)|\tilde{\Psi}_0^{s',\beta}(r)\rangle$, where $\tilde{\Psi}_0^{s,\gamma}(r)$ is the normalized edge wave function. Finding the diagonal and off-diagonal elements taking into account the spin-orbit coupling and finite warping coefficient, the effective edge Hamiltonian after rotating the Pauli matrices $\sigma_z \to \sigma_x$, and $\sigma_y \to \sigma_z$ takes the form

$$H_{\text{edge}}^{\gamma}(k_x) = E_0\mathcal{I} + D_0 k_x^2 \mathcal{I} + \lambda k_x^3 \sigma_x + \alpha k_x \sigma_z. \quad (10)$$

The details are provided in the Supplemental Material [74]. Adding the Zeeman energy term is equivalent to shifting the wave vector k by $k - E_Z/A$, which ensures that for the nonlinear current to be finite, the term $\propto \lambda$ is indispensable (this is a descendant of the well-known *warping* term in 2D systems). There will be no nonlinear response for this magnetic field orientation if $\lambda = 0$: hence an experimental measurement of a current at twice the applied frequency would immediately indicate that λ is finite. The edge energy dispersion for this model at the different Zeeman energy E_Z is demonstrated in Fig. 3. Interestingly, there is another case where the finite Zeeman energy along the σ_z opens a gap between conduction and valence bands in the dispersion, resulting the increase in the net current. In a similar way, we have derived the edge Hamiltonian for WTe_2 (Supplemental Material [74]).

Applications to topological materials.—We applied our general nonlinear theory for ballistic transport to various modeled systems. First, we consider the case for the inversion symmetric topological insulator Bi_2Se_3 whose edge dispersion is given by Eq. (10). Now, on adding the Zeeman energy term $\propto \sigma_z$, the origin in the momentum space gets shifted and the dispersion here is described by $\varepsilon = \sqrt{\lambda^2(k - E_Z/A)^6 + A^2k^2}\sigma_z$. We find that when $E_Z \to 0$, the second-order current vanishes as shown in Fig. 1 due to the vanishing $f_0^d = f_0(\varepsilon^+) - f_0(\varepsilon^-)$ at $k = 0$. However, the finite E_Z yields a nonzero second-order current, which increases at low energy and then saturates at low temperatures when the Zeeman energy and the chemical potential become equal, as depicted in Fig. 4. Nevertheless, as the temperature rises $j^{(2)}$ decreases due to the broadening of the delta function.

Second, for the WTe_2 model the edge dispersion is represented as $\varepsilon = \varepsilon_0\mathcal{I} + \varepsilon_3\sigma_z$, where $\varepsilon_0 = Dk^2$, and $\varepsilon_3 = \sqrt{(E_Z + Ak)^2 + (Ck + \lambda k^3)^2}$. Here the kinetic energy takes into account the particle hole asymmetry and the Zeeman term along $\hat{z}$ direction shifts the k points by an amount E_Z/A as mentioned earlier. In the same way as with Bi_2Se_3, we find that a finite λ leads to a finite value for the nonlinear current. This can be probed by varying the Zeeman energy and has behavior depicted in Fig. 1. Moreover, in both cases the nonlinearity can be increased by increasing the potential difference between the source and drain electrodes.

Third, for the edge states of quantum anomalous Hall insulators, the edge dispersion is $\varepsilon_0 = tk$, where t is a material dependent parameter. This degenerate dispersion for two bands gives the nonlinear current at the low temperature as $\delta(\mu)$, which survives only at zero chemical

potential. It is to be noted that $\mu = 0$ lies on the top of the valence band where the dispersion actually starts, thus in practice it will be rather challenging to observe the nonlinear current for quantum anomalous Hall edge states. Finally, for the HgTe edge states we find that $j^{(2)}$ vanishes with the linear wave vector Hamiltonian [81] along the $\hat{z}$ direction due to the absence of the warping and Zeeman field effects. The details are provided in the Supplemental Material [74].

In summary, we have shown that ballistic topological edge states exhibit a nonlinear response in the presence of inversion- and Kramers symmetry-breaking terms, which is nonzero on either side of a Zeeman gap, and provides an experimental probe ascertaining the presence of symmetry-breaking terms in the edge dispersion.

This work was supported by the Australian Research Council Centre of Excellence in Future Low-Energy Electronics Technologies (Project No. CE170100039). P. B. acknowledges the National Key Research and Development Program of China (Grant No. 2017YFA0303400), China postdoctoral science foundation (Grant No. 2019M650461) and NSFC Grant No. U1930402 for financial support.

[1] H. Zhang, C.-X. Liu, X.-L. Qi, X. Dai, Z. Fang, and S.-C. Zhang, Nat. Phys. **5**, 438 (2009).
[2] M. Z. Hasan and C. L. Kane, Rev. Mod. Phys. **82**, 3045 (2010).
[3] C.-X. Liu, X.-L. Qi, H. J. Zhang, X. Dai, Z. Fang, and S.-C. Zhang, Phys. Rev. B **82**, 045122 (2010).
[4] R.-L. Chu, W.-Y. Shan, J. Lu, and S.-Q. Shen, Phys. Rev. B **83**, 075110 (2011).
[5] I. Adagideli and G. E. W. Bauer, Phys. Rev. Lett. **95**, 256602 (2005).
[6] B. Yan and S.-C. Zhang, Rep. Prog. Phys. **75**, 096501 (2012).
[7] Z. K. Liu, B. Zhou, Y. Zhang, Z. J. Wang, H. M. Weng, D. Prabhakaran, S.-K. Mo, Z. X. Shen, Z. Fang, X. Dai, Z. Hussain, and Y. L. Chen, Science **343**, 864 (2014).
[8] B. Weber, Y. H. M. Tan, S. Mahapatra, T. F. Watson, H. Ryu, R. Rahman, L. C. L. Hollenberg, G. Klimeck, and M. Y. Simmons, Nat. Nanotechnol. **9**, 430 (2014).
[9] A. Farrell and T. Pereg-Barnea, Phys. Rev. B **93**, 045121 (2016).
[10] B. Yan and C. Felser, Annu. Rev. Condens. Matter Phys. **8**, 337 (2017).
[11] J. Wang and S.-C. Zhang, Nat. Mater. **16**, 1062 (2017).
[12] K. He, Y. Wang, and Q.-K. Xue, Annu. Rev. Condens. Matter Phys. **9**, 329 (2018).
[13] S.-Q. Shen, Topological Dirac and Weyl semimetals, in *Topological Insulators: Dirac Equation in Condensed Matter* (Springer Singapore, Singapore, 2017), pp. 207–229.
[14] W. Zhao, E. Runburg, Z. Fei, J. Mutch, P. Malinowski, B. Sun, X. Huang, D. Pesin, Y.-T. Cui, X. Xu, J.-H. Chu, and D. H. Cobden, arXiv:2010.09986 [Phys. Rev. X (to be published)].
[15] M. S. Lodge, S. A. Yang, S. Mukherjee, and B. Weber, Adv. Mater. **33**, 2008029 (2021).
[16] Y. Wang, S.-S. Wang, Y. Lu, J. Jiang, and S. A. Yang, Nano Lett. **16**, 4576 (2016).
[17] J. L. Collins, A. Tadich, W. Wu, L. C. Gomes, J. N. B. Rodrigues, C. Liu, J. Hellerstedt, H. Ryu, S. Tang, S.-K. Mo, S. Adam, S. A. Yang, M. S. Fuhrer, and M. T. Edmonds, Nature (London) **564**, 390 (2018).
[18] B. Scharf, A. Matos-Abiague, I. Žutić, and J. Fabian, Phys. Rev. B **91**, 235433 (2015).
[19] H. Rostami and V. Juričić, Phys. Rev. Research **2**, 013069 (2020).
[20] G. A. Nemnes, U. Wulf, and P. N. Racec, J. Appl. Phys. **96**, 596 (2004).
[21] J. Fabian and I. Žutić, Phys. Rev. B **69**, 115314 (2004).
[22] B. Huang, D. J. Monsma, and I. Appelbaum, Appl. Phys. Lett. **91**, 072501 (2007).
[23] L. A. Wray, Nat. Phys. **8**, 705 (2012).
[24] L. Vicarelli, M. S. Vitiello, D. Coquillat, A. Lombardo, A. C. Ferrari, W. Knap, M. Polini, V. Pellegrini, and A. Tredicucci, Nat. Mater. **11**, 865 (2012).
[25] R. Cheng, M. W. Daniels, J.-G. Zhu, and D. Xiao, Sci. Rep. **6**, 24223 (2016).
[26] R. Landauer, Philos. Mag. **21**, 863 (1970).
[27] R. Landauer, Z. Phys. B Condens. Matter **68**, 217 (1987).
[28] A. I. Larkin and D. E. Khmel'nitskii, Sov. Phys. JETP **64**, 1075 (1986).
[29] P. F. Bagwell and T. P. Orlando, Phys. Rev. B **40**, 1456 (1989).
[30] Y. Meir and N. S. Wingreen, Phys. Rev. Lett. **68**, 2512 (1992).
[31] H. M. Pastawski, Phys. Rev. B **46**, 4053 (1992).
[32] R. Landauer, Phys. Scr. **T42**, 110 (1992).
[33] S. Datta, *Physics of Low-Dimensional Semiconductor Structures*, edited by P. Butcher and M. P. March, Norman H. Tosi (Springer, Boston, MA, 1993), pp. 299–331.
[34] M. Büttiker and T. Christen, *Theory of Transport Properties of Semiconductor Nanostructures*, edited by E. Schöll (Springer, Boston, MA, 1998), pp. 215–248.
[35] S. Datta, *Quantum Transport: Atom to Transistor* (Cambridge University Press, Cambridge, England, 2005).
[36] F. Green and M. P. Das, J. Phys. Condens. Matter **12**, 5251 (2000).
[37] W. Liang, M. Bockrath, D. Bozovic, J. H. Hafner, M. Tinkham, and H. Park, Nature (London) **411**, 665 (2001).
[38] C. Jeong, R. Kim, M. Luisier, S. Datta, and M. Lundstrom, J. Appl. Phys. **107**, 023707 (2010).
[39] I. Knez, R.-R. Du, and G. Sullivan, Phys. Rev. Lett. **107**, 136603 (2011).
[40] V. Cheianov and L. I. Glazman, Phys. Rev. Lett. **110**, 206803 (2013).
[41] X. Wang and Y. Kruglyak, J. Nanosci. Nanotechnol. **2014**, 725420 (2014).
[42] I. Knez, C. T. Rettner, S.-H. Yang, S. S. P. Parkin, L. Du, R.-R. Du, and G. Sullivan, Phys. Rev. Lett. **112**, 026602 (2014).
[43] L. Du, I. Knez, G. Sullivan, and R.-R. Du, Phys. Rev. Lett. **114**, 096802 (2015).
[44] T. Li, P. Wang, H. Fu, L. Du, K. A. Schreiber, X. Mu, X. Liu, G. Sullivan, G. A. Csáthy, X. Lin, and R.-R. Du, Phys. Rev. Lett. **115**, 136804 (2015).

[45] Z. Fei, T. Palomaki, S. Wu, W. Zhao, X. Cai, B. Sun, P. Nguyen, J. Finney, X. Xu, and D. H. Cobden, Nat. Phys. **13**, 677 (2017).
[46] D. E. Khmelnitskii and A. I. Larkin, Phys. Scr. **1986**, T14 (1986).
[47] T. Christen and M. Büttiker, Europhys. Lett. **35**, 523 (1996).
[48] A. M. Song, A. Lorke, A. Kriele, J. P. Kotthaus, W. Wegscheider, and M. Bichler, Phys. Rev. Lett. **80**, 3831 (1998).
[49] J. Q. You, C.-H. Lam, and H. Z. Zheng, Phys. Rev. B **62**, 1978 (2000).
[50] I. Shorubalko, H. Q. Xu, I. Maximov, P. Omling, L. Samuelson, and W. Seifert, Appl. Phys. Lett. **79**, 1384 (2001).
[51] S. Reitzenstein, L. Worschech, P. Hartmann, M. Kamp, and A. Forchel, Phys. Rev. Lett. **89**, 226804 (2002).
[52] M. L. Polianski and M. Büttiker, Phys. Rev. B **76**, 205308 (2007).
[53] I. Safi and P. Joyez, Phys. Rev. B **84**, 205129 (2011).
[54] C.-Z. Chang, W. Zhao, D. Y. Kim, P. Wei, J. K. Jain, C. Liu, M. H. W. Chan, and J. S. Moodera, Phys. Rev. Lett. **115**, 057206 (2015).
[55] Y. Korniyenko, O. Shevtsov, and T. Löfwander, Phys. Rev. B **93**, 035435 (2016).
[56] H. Rostami and M. Polini, Phys. Rev. B **97**, 195151 (2018).
[57] C. Texier and J. Mitscherling, Phys. Rev. B **97**, 075306 (2018).
[58] S. Mardanya, U. Bhattacharya, A. Agarwal, and A. Dutta, Phys. Rev. B **97**, 115443 (2018).
[59] F. Ildarabadi and R. Farghadan, Phys. Rev. B **103**, 115424 (2021).
[60] C. Beenakker and H. van Houten, Solid State Phys. **44**, 1 (1991).
[61] B. L. Altshuler and D. E. Khmelnitskii, Sov. Phys. JETP **42**, 359 (1985).
[62] R. A. Webb, S. Washburn, and C. P. Umbach, Phys. Rev. B **37**, 8455 (1988).
[63] M. Buttiker, J. Phys. Condens. Matter **5**, 9361 (1993).
[64] J. S. Thakur, F. Green, and M. P. Das, Int. J. Mod. Phys. B **18**, 1479 (2004).
[65] D. Sánchez and M. Büttiker, Phys. Rev. Lett. **93**, 106802 (2004).
[66] A. Löfgren, C. A. Marlow, I. Shorubalko, R. P. Taylor, P. Omling, L. Samuelson, and H. Linke, Phys. Rev. Lett. **92**, 046803 (2004).
[67] S. Datta, *Lessons from Nanoelectronics: A New Perspective on Transport*, Lessons from nanoscience No. pt. 1 (World Scientific, Singapore, 2017).
[68] L. k. Shi and J. C. W. Song, Phys. Rev. B **99**, 035403 (2019).
[69] S. Sun, Z. Song, H. Weng, and X. Dai, Phys. Rev. B **101**, 125118 (2020).
[70] T. Morimoto and N. Nagaosa, Sci. Rep. **8**, 2973 (2018).
[71] A. Arora, L. k. Shi, and J. C. W. Song, Phys. Rev. B **102**, 161402(R) (2020).
[72] P. Carruthers and F. Zachariasen, Rev. Mod. Phys. **55**, 245 (1983).
[73] F. T. Vasko and O. E. Raichev, *Quantum Kinetic Theory and Applications* (Springer-Verlag, New York, 2005).
[74] See Supplemental Material at http://link.aps.org/supplemental/10.1103/PhysRevLett.127.206801 for details on (i) density matrix theory of 1D ballistic transport where we discuss the linear-order and second-order cases, (ii) derivation for the edge state Hamiltonian for different systems, and (iii) ballistic transport for different edge state Hamiltonians.
[75] D. Culcer and Q. Niu, Phys. Rev. B **74**, 035209 (2006).
[76] D. Culcer, M. E. Lucassen, R. A. Duine, and R. Winkler, Phys. Rev. B **79**, 155208 (2009).
[77] A. Sekine, D. Culcer, and A. H. MacDonald, Phys. Rev. B **96**, 235134 (2017).
[78] D. Culcer, A. Sekine, and A. H. MacDonald, Phys. Rev. B **96**, 035106 (2017).
[79] M. P. Marder, *Condensed Matter Physics* (John Wiley and Sons, Ltd, New York, 2010), pp. 453–481.
[80] L. Fu, Phys. Rev. Lett. **103**, 266801 (2009).
[81] M. V. Durnev and S. A. Tarasenko, Phys. Rev. B **93**, 075434 (2016).